Viscoelastic Model for the Plastic Flow of Amorphous Solids under Energetic Ion Bombardment

H. Trinkaus
Institut für Festkörperforschung, Forschungszentrum Jülich GmbH, D-52425 Jülich, Germany

A. I. Ryazanov
Russian Research Centre "Kurchatov Institute," 123182 Moscow, Russia
(Received 20 September 1994)

Under energetic ion bombardment, amorphous solids show substantial plastic flow in the form of anisotropic growth. This is attributed to the relaxation of shear stresses coupled to the thermal expansion in cylindrical thermal spikes induced by intense electronic excitations and to the subsequent freezing-in of the associated strain increment upon cooling down. An asymptotic growth rate at high electronic stopping power and low irradiation temperature is derived which correlates the growth rate with a few simple material parameters without introducing any adjustable free parameter. Good agreement with measurements justifies the basic assumptions of the model.

PACS numbers: 61.43.–j, 61.80.Jh, 65.70.+y

Presently, bombardment of solid materials with energetic ions is becoming increasingly important in material engineering, particularly in microelectronics where it is used to modify surfaces, to dope and to change the state and the microstructure of surface layers, or to synthesize buried epitaxial layers [1]. In investigating the effects of energetic ion bombardment on free and substrate bound amorphous thin films, two interesting sets of observations have been made recently: (1) For sufficiently high electronic stopping powers ($\gtrsim$1 keV/nm) [2] and sufficiently low temperatures, stress free amorphous films showed unsaturable plastic flow in the form of anisotropic growth at negligible density change in which the ion beam seems to act like a hammer rolling out the sample in the directions perpendicular to the beam. The changes in the specimen surfaces are typically between 10^{-19} and 10^{-18} m^2 per penetrating ion. In some but not in all cases, a certain incubation fluence was found to be required for this type of dimensional change [3–6]. (2) Under ion bombardment, stressed amorphous samples showed surprisingly high stress relaxation and creep rates, respectively, being larger by orders of magnitude than those found in metals under otherwise comparable conditions [6–10].

For metals, it is generally accepted that irradiation creep, for instance, is due to the stress-induced preferential absorption (SIPA) of self-interstitial atoms by favorably oriented dislocations [11]. Anisotropic creep and growth of amorphous solids under ion bombardment can certainly not be understood in terms of such a simple defect reaction kinetics. Nevertheless, attempts have been made to use some kind of reaction kinetics to explain these phenomena [12,13]. The growth of amorphous solids under energetic ion bombardment, for instance, has been attributed to the production of "shear units" representing some "mechanical polarization" of the material which is assumed to "trigger irreversible shear transformations" [3–6]. Recently, a viscoelastic model for the creep of ion bombarded amorphous solids has been suggested in which stress relaxation in locally heated regions and the freezing-in of the associated strain increment upon cooling down are assumed [14]. Similarly, the anisotropic growth phenomenon has been attributed very recently to radial material fluxes in the hot region around ion tracks [15].

In the present paper, the anisotropic growth of amorphizing and amorphous solids is discussed in terms of such a viscoelastic model. A simple asymptotic expression for intense electronic excitations and low irradiation temperatures is derived and compared with experimental results. An analogous approach allows one to successfully model irradiation creep which is presented elsewhere [16].

It is useful here to briefly recall the basic processes associated with the interaction of an energetic ion with the electrons of the target which represents the dominant contribution to the stopping power at high ion energies ($\gtrsim$1 MeV). The first step occurring in less than 10^{-16} s is electronic excitation and ionization along the track of the projectile. These processes are perhaps followed by a "Coulomb explosion" by which part of the energy is transferred to the atomic subsystem [3]. Local thermalization in the electronic system will be complete at about 10^{-14} s. Heat transfer from the electronic to the atomic subsystem becomes substantial between 10^{-14} and 10^{-12} s depending on the magnitude of the coupling between both subsystems [17]. For intense electronic excitations and efficient electron-phonon coupling, a cylindrical region around the track of the ion may become fluid in the sense that any thermally induced shear stress would relax in this region. For an electronic stopping power of a few keV/nm, the fluid zone reaches its maximum extension of some nm within some ps [17]. In this stage, the system has virtually "forgotten" most of the features of the preceding processes. After about 100 ps the region has virtually

 0031-9007/95/74(25)/5072(4)$06.00

cooled down to ambient temperatures but generally in a transformed state due to the relaxation of shear stresses during the spike phase.

Thermal spikes may also occur in displacement cascades [18,19]. There is, however, a difference between displacement cascades and electronic excitations which is crucial in the present context. Spikes resulting from displacement cascades are approximately spherical, whereas spikes induced by electronic excitations are characterized by a cylindrical geometry. The importance of this difference is schematically illustrated in Fig. 1. Consider a spherical or cylindrical piece of volume V_0 (inner thin lines in Fig. 1) cut out of an isotropic material. Upon heating by a temperature difference ΔT, such a piece would transform to a larger but geometrically similar piece of volume $V_0(1 + \alpha\Delta T)$ (outer thin line in Fig. 1) where α is the thermal volume expansion coefficient (which is assumed here to be temperature independent). The "stress free" or "transformation" strain [20] defined by this procedure is isotropic and given by trace $\underline{\underline{\epsilon}}^T = \alpha\Delta T$. Now consider the piece to be squeezed into the hole from where it originates. While the surrounding matrix would yield somewhat, thus assuming strain and stress fields of pure shear character, the resulting "constrained" volume of the transformed piece (thick line in Fig. 1) would be compressed to a size between that of the original volume and that of the stress free transformation volume. The elastic strain in this inclusion is uniform and given by the corresponding difference between the constrained and the stress free strain: $\underline{\underline{\epsilon}}^I = \underline{\underline{\epsilon}}^C - \underline{\underline{\epsilon}}^T$ [20].

At this point, the geometry of the inclusion becomes important. In the case of a spherical inclusion, the constrained strain as well as the stress free strain and hence also the elastic strain and stress within the inclusion are hydrostatic. In the case of a nonspherical ellipsoidal inclusion and particularly in the limiting case of a long cylindrical inclusion (on which we focus interest in the following), the constrained strain and hence also the elastic strain and stress within the inclusion are no longer hydrostatic but contain shear components. When the length of the cylindrical inclusion is much larger than its diameter, $\ell \gg d$, the surroundings yield elastically in the transversal directions, $\epsilon_{11}^C = \epsilon_{22}^C \neq 0$, but virtually prevent any extension of the inclusion in the longitudinal direction, $\epsilon_{33}^C \to 0$. For sufficiently high temperatures, the shear stress in the inclusion corresponding to the difference $\epsilon_{11,22}^C - \epsilon_{33}^C$ will relax and in amorphous materials the increment of shear strain in the transformation strain associated with this stress relaxation can freeze-in. (It can be shown that this holds even for thermal spikes penetrating a whole film [21].)

We postulate here that anisotropic growth of amorphizing and amorphous materials being subject to intense electronic excitations is due to the efficient relaxation of shear stresses within cylindrical thermal spike regions induced by the thermal dilatation and to the freezing-in of the associated shear strain increments. The sequence of events occurring during local heating and cooling is schematically illustrated in Fig. 2. Consider a piece of material of total volume V in which a cylindrical region of time-dependent volume V^* is subjected to a heating and cooling history, $T(t)$. At the beginning, the stress free dilatation $\alpha\Delta T$, which follows the temperature history, is coupled with a constrained elastic shear strain $\tilde{\epsilon}^C$ and a shear stress $\tilde{\sigma}^I = 2\mu\tilde{\epsilon}^I = 2\mu\tilde{\epsilon}^C$ within the spike where μ is the shear modulus of the material. Below a certain critical temperature T^* ("flow temperature") which is equal to the melting temperature for crystalline solids, $T^* = T_m$, shear stress relaxation is negligible. In this stage, the average strain over the whole volume V is dilatational and given by $\langle \mathrm{tr}\underline{\underline{\epsilon}} \rangle = \langle \mathrm{tr}\underline{\underline{\epsilon}}^T \rangle V^*/V = \alpha\langle\Delta T\rangle V^*/V$. Above the flow temperature,

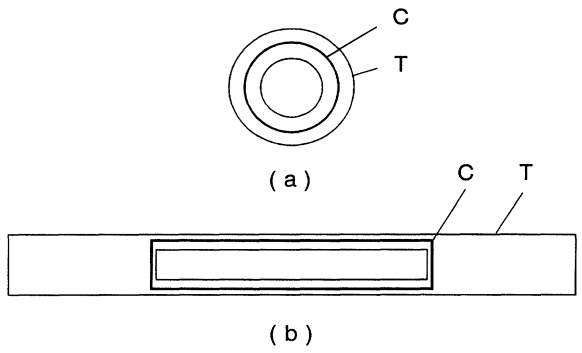

FIG. 1. Schematic illustration of the effect of the constraint imposed on a heated region by its cool surroundings (a) for a spherical and (b) for a long cylindrical region. The inner thin lines, the outer thin lines, and the medium thick lines indicate the boundaries in the initial state, the heated stress free state (T), and the heated constrained state (C), respectively. In case (a), the boundaries C and T are geometrically similar and the corresponding states inside C and T are both isotropic dilatations. In case (b), C and T are not geometrically similar and the isotropic dilatation of T is coupled with a shear strain inside C.

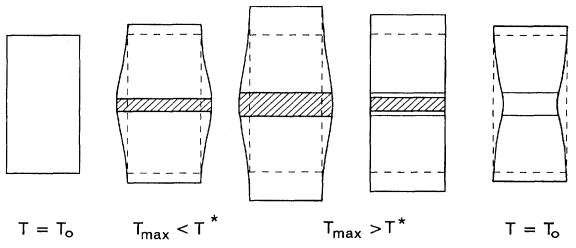

FIG. 2. Schematic illustration of the sequence of events induced by a cylindrical thermal spike in an amorphous solid. Below the flow temperature T^* the strain is dilatational on the average. Above T^* the shear stress in the hot region relaxes thus providing a certain shear strain increment. In a crystalline solid this process would be reversed by recrystallization whereas in an amorphous solid the relaxed state will freeze-in upon cooling down of the spike.

the local shear stress within the thus fluid region, $\tilde{\sigma}^l$, begins to relax (and the pressure begins to equalize), whereas shear stress relaxation in the cooler surroundings remains negligible. Upon (quasistatic) shear stress relaxation, $\tilde{\sigma}_l = 2\mu(\tilde{\epsilon}^C - \tilde{\epsilon}^T) \rightarrow 0$, a shear component in the stress free strain, $\tilde{\epsilon}^T = \tilde{\epsilon}^C$, is induced in the thermal spike region which thus contributes an increment of strain, $\Delta\tilde{\epsilon} = \tilde{\epsilon}^T V^*/V$, to the total volume.

In crystalline materials, however, recrystallization results in an inversion of the liquid state relaxation process and the initial state is essentially restored (ideal epitaxy). Thus, in recrystallizing solids transient local melting is associated with transient strain increments. In amorphous materials, on the other hand, the relaxed hot region has the same atomic structure as the stressed environment and the strain increment associated with stress relaxation can therefore freeze-in. Upon cooling down, the thermal expansion along the ion track is reversed but the strain increment associated with the preceding stress relaxation remains. In the stress free state, the quenched ion track would represent a plastically deformed cylindrical rod of reduced length and correspondingly enlarged cross section. A track penetrating a thin film acts like a tensioned string tight between the two surfaces of the film. The stress in this region is compensated by counterstresses in the surrounding regions. Thus, *each track as a whole represents a "shear strain unit."* In its region, the concentration of atomic shear strain units introduced previously is virtually 100% [4].

For pronounced thermal spikes (what this means is briefly discussed below) it can be shown that the superheated ($T \geq T^*$) and quickly relaxing core volume V^* is relatively well defined, meaning that the boundary between it and its surroundings is relatively sharp [21]. Accepting this in the present Letter, we can immediately write the following simple relation for the shear strain rate resulting from the perfect quenching to low irradiation temperature of pronounced cylindrical spikes occuring at high electronic stopping power:

$$\dot{\tilde{\epsilon}} = \langle\tilde{\epsilon}^T\rangle(V^*/Q)q = \langle\tilde{\epsilon}^T\rangle(V^*/Q)\phi S_e', \qquad (1)$$

where $\langle\tilde{\epsilon}^T\rangle$ is the average stress free shear strain in a frozen thermal spike track, Q is the average heat per spike, q is the average overall heat production density by spikes, ϕ is the particle flux density, and S_e' is the part of the electronic stopping power put into "pronounced spikes" in the atomic subsystem. The remaining tasks are to relate the volume efficiency of the deposited heat (V^*/Q) to thermal properties of the material and the stress free shear strain $\tilde{\epsilon}^T$ to the thermally induced shear stress.

The boundary of V^* is defined by the surface where the maximum temperature equals the flow temperature T^*. Assuming a temperature independent specific heat we find for a Gaussian heat distribution $V^* = Q/e\rho C\Delta T^*$, where ρ is the mass density, C is the specific heat per unit mass, and ΔT^* is the difference between the irradiation and the flow temperature. The determination of T^* is a more complicated problem and beyond the scope of this Letter. Here, we only note that its value is around the melting temperature [21].

The relation between the stress free shear strain $\tilde{\epsilon}^T$ freezing-in below T^* and the thermal expansion at $T = T^*$ follows from the theory of elastic inhomogeneities in elastically isotropic media as evaluated by Eshelby for ellipsoidal elastic inclusions [20]. Taking the third coordinate to be parallel to the cylinder axis we use $\langle\tilde{\epsilon}^T\rangle = \langle\tilde{\epsilon}^C\rangle$ for the relaxed state and $\langle\tilde{\epsilon}^C\rangle \propto \langle\epsilon^C_{11,22} - \epsilon^C_{33}\rangle = 3\langle\epsilon^C_{11,22}\rangle = -3\langle\epsilon^C_{33}\rangle/2 = A\alpha\langle\Delta T\rangle$, where $A = (1 + \nu)/(5 - 4\nu)$ is the coupling coefficient between the corresponding strains depending only upon Poisson's ratio ν. The temperature is to be averaged at a given time over the region where $T \geq T^*$ and over all the sizes assumed by such regions during the cooling down process. For cylindrical heat diffusion we find $\langle\Delta T\rangle = 1.16\alpha(T^* - T_0)$. Using $V^*/Q = [e\rho C(T^* - T_0)]^{-1}$ we may then write Eq. (1) as

$$\dot{\epsilon}_{11} = \dot{\epsilon}_{22} = -\dot{\epsilon}_{33}/2 = (1.16/3e)[(1 + \nu)/(5 - 4\nu)] \times (\alpha/\rho C)\phi S_e'. \qquad (2)$$

The temperature difference (and with this the flow temperature) has canceled in this linear approximation since it is contained both in the thermal expansion as well as in the heat deposited in the spike. Note that an approximately spherical displacement cascade would not contribute to the deformation rate since in this case the thermal expansion would not couple with a local shear stress.

According to the approximation represented by Eq. (2) the strain rate depends linearly upon ϕ and S_e' without any incubation fluence. This suggests to introduce a normalized strain rate $\dot{E} = \phi^{-1}d\dot{\epsilon}/dS_e'$ which depends only on the material parameters ν, α, and ρC. For typical thermal expansion coefficients around $\alpha = 10^{-5}$ K^{-1} and high temperature specific heats of $3k$ per atom (k is Boltzmann's constant) $\dot{E}$ is of the order of 3×10^{-13} m^3/J in agreement with experimental values for high electronic stopping powers (>5 keV/nm) and low irradiation temperatures (<150 K) [4,5]. Figure 3 shows a correlation between experimental and theoretical values of $\dot{E}$ for this limiting case (assuming $S_e = S_e'$) for materials for which the relevant data are sufficiently well known [22]. The correlation is surprisingly good in view of the limited accuracy of the data and appears to be universal. The fact that in most cases $\dot{E}_{\text{exp}} < \dot{E}_{\text{theor}}$ is probably due to long-ranging electronic energy transport ($S_e' < S_e$).

Equation (2) represents an asymptotic approximation for pronounced cylindrical thermal spikes and low irradiation temperatures where virtually all atomic motions are frozen-in upon quenching, and its applicability is correspondingly limited. A necessary condition for anisotropic growth, for instance, is that the thermal spike around the track of an ion forms a coherent cylindrical region and does not break up in a "string of elastically independent perls."

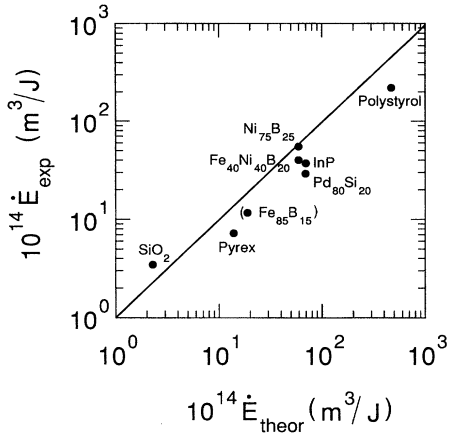

FIG. 3. Correlation between experimental and theoretical values of the normalized strain rate $\dot{E} = \phi^{-1} d\dot{\epsilon}/dS_e$ using for $\dot{\epsilon}$ experimental results for high electronic stopping power S_e and low temperature, and Eq. (2) with $S_e' = S_e$, respectively [22]. Line: ideal correlation. The point for $Fe_{85}B_{15}$ is uncertain because of magnetostriction effects.

The validity of Eq. (2) requires, in addition, that the maximum temperature in the atomic system is clearly above the critical flow temperature ($T_{max} = eT^*$ for a cylindrical Gaussian heat distribution). By these requirements, a minimum electronic stopping power for anisotropic growth is defined.

The validity of Eq. (2) is also limited by the condition that the strain increment associated with stress relaxation is efficiently frozen-in upon quenching. The extremely fast heating and quenching processes may, however, result in a local reduction of the viscosity and of the corresponding glass temperature in the thermal spike regions. Around temperatures where the stress relaxation time in the quenched spikes becomes comparable with the characteristic time for the overlap of these regions, i.e., around the glass temperature of the modified amorphous state, the quenched-in strain increment will partially recover and anisotropic growth will decrease with increasing temperature. We predict here that around this temperature growth will partially recover upon homogenization of the inhomogeneous stress distribution. For anisotropic growth, an incubation fluence will be required if the electronic stopping power used is subcritical in the virgin amorphous state but supercritical in the state modified by irradiation. We predict that any incubation fluence will disappear at sufficiently high electronic stopping powers.

We thank Dr. S. Klaumünzer for encouraging discussions and for providing the correlation shown in Fig. 3.

[1] Proceedings of the International Conferences on Ion Beam Modifications of Materials; see, for instance, Nucl. Instrum. Methods Phys. Res., Sect. B **80/81** (1993).
[2] Heavy ions with energies in the MeV range are close to the lower limit.
[3] S. Klaumünzer, Ming-dong Hou, and G. Schumacher, Phys. Rev. Lett. **57**, 850 (1986).
[4] Ming-dong Hou, S. Klaumünzer, and G. Schumacher, Phys. Rev. B **41**, 1144 (1990).
[5] S. Klaumünzer, Radiat. Eff. **110**, 79 (1989).
[6] A. Audouard, E. Balanzat, J. C. Jousset, D. Lesueur, and L. Thomé, J. Phys. Condens. Matter **5**, 995 (1993).
[7] C. Hardtke, W. Schilling, and H. Ullmaier, Nucl. Instrum. Methods Phys. Res., Sect. B **59/60**, 377 (1991).
[8] C. A. Volkert, J. Appl. Phys. **70**, 3521 (1991).
[9] E. Snoeks, A. Polman, and C. A. Volkert, Appl. Phys. Lett. **65**, 2487 (1994).
[10] Z. Zhu and P. Jung, Nucl. Instrum. Methods Phys. Res., Sect. B **91**, 269 (1994).
[11] P. T. Heald and M. V. Speight, Philos. Mag. **29**, 1075 (1974); R. Bullough and J. R. Willis, Philos. Mag. **31**, 855 (1975); W. G. Wolter and M. J. Ashkin, J. Appl. Phys. **47**, 791 (1976).
[12] C. H. de Novion and A. Barbu, Solid State Phenomena **30 & 31**, 277 (1993).
[13] G. Szenes, Mater. Sci. For. **97–99**, 647 (1992).
[14] A. Barbu, M. Bibole, R. le Hazit, S. Bouffard, and J. C. Ramillon, J. Nucl. Mater. **165**, 217 (1989).
[15] A. I. Ryazanov, A. E. Volkov, and S. Klaumünzer, Phys. Rev. B **51**, 12 107 (1995).
[16] H. Trinkaus, J. Nucl. Mater. **223**, 169 (1995).
[17] Z. G. Wang, C. Dufour, E. Paumier, and M. Toulemonde, J. Phys. Condens. Matter **6**, 6733 (1994).
[18] T. Diaz de la Rubia and M. W. Guinan, Phys. Rev. Lett. **66**, 2766 (1991); A. J. E. Foreman, W. J. Phythian, and C. A. English, Philos. Mag. A **66**, 671 (1992).
[19] In the case of heavy ions with energies in the MeV range both types of spikes may be important.
[20] J. D. Eshelby, Proc. R. Soc. London Sect. A **241**, 376 (1957).
[21] H. Trinkaus (to be published).
[22] S. Klaumünzer (private communication); (to be published).